



1 Article

2 **Efficient and eco-friendly mechanical milling**
3 **preparation of anatase/rutile TiO₂-Glucose composite**
4 **with energy gap enhancement**

5 **Imane Ellouzi** ^{1,*} and **Hicham Abou Oualid** ^{2,*}

6 ¹ Faculty of Sciences, Rabat, Morocco; im.ellouzi@gmail.com

7 ² Faculty of Sciences and Technologies, Mohamedia, Morocco; hicham.abououalid@gmail.com

8 * Correspondence: hicham.abououalid@gmail.com; Tel.: +212 66 777 2424

9 Academic Editor: name

10 Received: date; Accepted: date; Published: date

11 **Abstract:** In the current study, Anatase/rutile TiO₂ and Anatase/rutile TiO₂@Glucose composites were
12 successfully prepared by a simple method using mechanical technique. The as-prepared composite
13 materials powders were characterized by Powder X-ray diffraction analysis (PXRD), Scanning
14 electronic microscopy (SEM) and Solid-state UV-visible spectroscopy. X-ray patterns showed the
15 fractional phase transformation from TiO₂ anatase to rutile. SEM observations revealed that the
16 particle shape was affected by ball milling process. EDS analysis exhibits quantitatively the elemental
17 composition of Ti and O. UV-Visible spectroscopy confirmed that the bandgap is slightly affected
18 using Tauc.

19

20 .

21 **Keywords:** Anatase/rutile, composite, TiO₂, Mechanical technique, TiO₂-Glucose and gap energy.

22

23

24 **1. Introduction**

25 Titanium dioxide (TiO₂) is among the most useful materials for many applications due to its
26 nontoxicity, low cost, physical and chemical stability, availability and optical properties [1]. Titanium
27 dioxide (TiO₂) exists as three different phases; anatase, rutile and brookite [2]. The band gaps (3–3.2
28 eV) of TiO₂ semiconductors, absorb just from the UV region of the solar spectrum. Several processing
29 techniques have been used to synthesize TiO₂ particles, coprecipitation [3], and sol-gel [4] etc.
30 Among these methods, high energy milling is an effective and a general term describing mechanical
31 action by hard surfaces on a material and has the advantages to break up the particles and reduce
32 their particle size, simple and easy. The effect of various ball milling parameters on the properties of
33 the bulk samples, relatively inexpensive, and applicable to any class of materials which can be easily
34 scaled up to large quantities [5]. Ball milling has attracted considerable attention and is an effective
35 physical mechanical milling synthesis method owing to the relatively low installation cost, the large
36 number of particles can be easily obtained by solely grinding bulk materials in a milling vessel with

37 milling balls, and capability to treat materials of all hardness degrees. However, few studies have
38 been reported on the production of TiO₂ particles by ball milling [6-16]. The milling is a simple and
39 an easy method for increasing the particle size from macro to nanometric level. In addition, ball
40 milling is one of the effective mechanical milling processes and the milling time plays very important
41 role. During ball milling, many parameters could be studied to decrease the particles size such as the
42 powder-to-ball weight ratio, high speed rotating grinding machine, time of mechanical process [17].
43 The purpose of this work is to modify the particles size and shape, crystal structure, optical properties
44 as well as phase transformation of TiO₂ using high energy ball milling process. We have also
45 investigated the effect of Glucose on the morphological and optical properties of milled anatase-rutile
46 TiO₂ composites, as well as the gap energy of as-prepared composite materials.

47

48 **2. Materials and Methods**

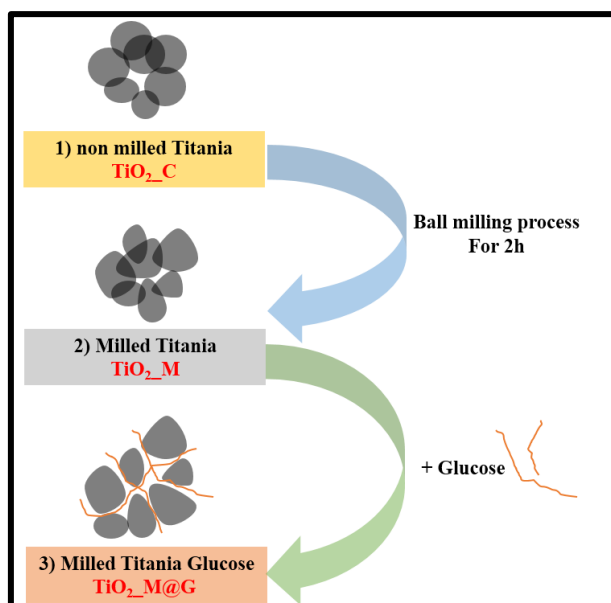
49 *2.1 Materials and Reagents*

50 TiO₂ powder and glucose were purchased from Aldrich and used without any further purification.
51 Commercial TiO₂ (TiO₂_C) powders with an average crystallite size of about 134 nm was used as
52 precursor. Ball milling (BM) was carried out using a high energy planetary ball mill machine (Retsch
53 PM100, Germany).

54 *2.2 Synthesis procedure*

55 All milled samples followed the same experiment conditions: revolution speed fixed at 450 rpm;
56 room temperature; stopped periodically for every 30 minutes and then resumed for 30 min. The
57 milling time period was 2h and the mass ratio of stainless steel balls to TiO₂ was set at 20: 1. After ball
58 milling process, the color of TiO₂ powders has become gray-blue. The changed of color from yellow
59 to gray could be explained by the fact that TiO₂ got its proper structure of its oxide phase. Gray color
60 after calcination is unchanged which confirm that the powders were not be contaminated
61 (incorporation of zirconia or other impurity). Furthermore, the color change is from reduction
62 (formation of oxygen vacancies) which was proved by EDS analysis. Thus, the color comes from the
63 material itself. Then, 1 g of glucose was dissolved in deionized water and agitated until miscibility
64 and added dropwise into milled TiO₂ solution and aged all night. At the end of the reaction, the final
65 products were filtered and washed with deionized water, ethanol and dried at 80°C for 24h in a
66 vacuum oven to give TiO₂-M@G composite (fig. 1).

67



68

69

Figure 1. Schematic illustration of synthetic chemical process of composite materials

70

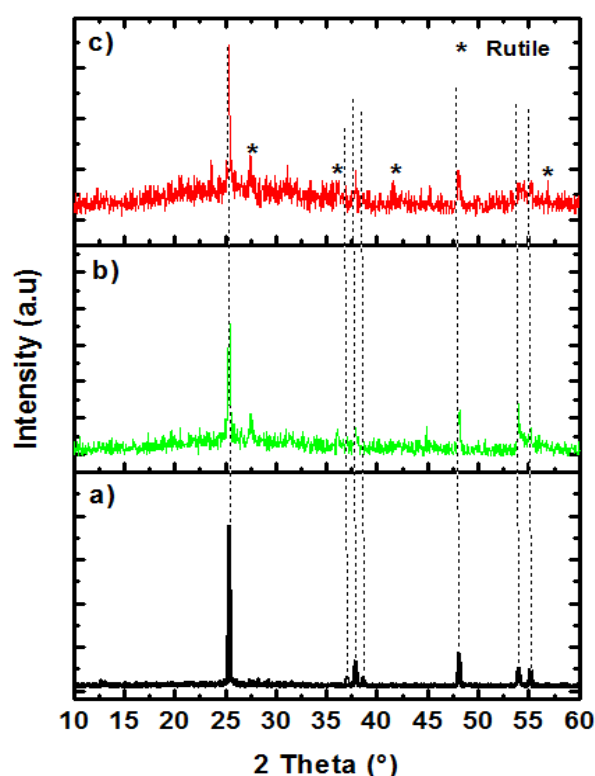
71 2.3 Characterizations and techniques

72 Powder X-ray diffraction (PXRD) patterns were obtained at room temperature on a Bruker AXS D-8
73 diffractometer using Cu-K α radiation in Bragg-Brentano geometry (θ -2 θ). The SEM and EDS analysis
74 was recorded by (JEOLJSM-IT100, Japan) with gold sputter coating (JEOL Smart Coater, Japan). The
75 UV-vis diffuse reflectance spectrum was obtained using Perkin-Elmer Lambda 35 UV-Visible
76 spectrophotometer.

77

78 3. Results and Discussion

79 Figure 2 displays the comparison of XRD patterns of pure anatase ($\text{TiO}_2\text{-C}$), milled TiO_2 ($\text{TiO}_2\text{-M}$) and
80 milled $\text{TiO}_2\text{@Glucose}$ ($\text{TiO}_2\text{-M@G}$). The major reflections of non-milled material ($\text{TiO}_2\text{-C}$) exhibits a
81 major peak at 2θ value of 25.3° , 37.8° , 48.0° , 53.7° , 54.9° and 62.5° , which corresponding to anatase (1
82 0 1), (0 0 4), (2 0 0), (1 0 5), (2 1 1) and (2 0 4) crystal planes (JCPDS 21-1272), respectively. Figure 2b
83 and 2c exhibits diffraction peaks at 2θ of 25.2° , 27.2° , 35.9° , 37.8° , 41.2° , 47.8° , 54.2° , 55.2° , and 62.4° ,
84 which can be indexed to the TiO_2 anatase and rutile composite. This result indicates that there is a
85 phase transformation during the milling from anatase to rutile. It could be assigned to the enormous
86 amount of heat induced by high energy which if not controlled and could thermally transforms
87 anatase to rutile phase or to the difference in speeds between the balls and grinding jars which could
88 produce an interaction between frictional and impact forces, releasing high dynamic energies [18].



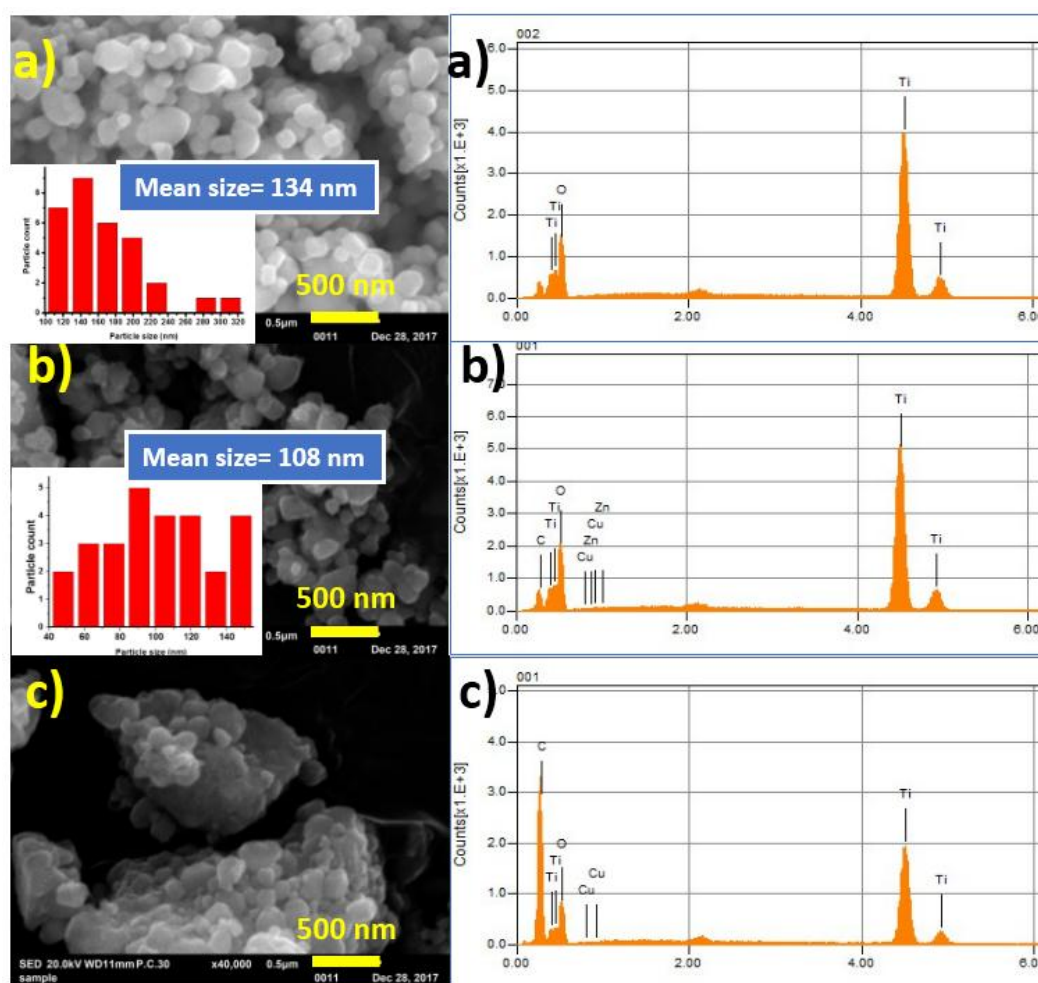
89
90

Figure 2. PXRD patterns analysis of $\text{TiO}_2\text{-C}$ (a), $\text{TiO}_2\text{-M}$ (b) and $\text{TiO}_2\text{-M@G}$ (c)

91 It was observed a decrease in the intensity of the Bragg peak of the crystalline phase, while a broad,
92 amorphous phase signal emerged for milled samples. A decrease in the intensities of peaks was
93 observed could be due to the decrease in the grain size and lattice distortion. These effects could be
94 assigned to the change in the particle size and internal structure of TiO_2 crystallite induced by ball
95 milling process. It has been reported by some authors that the increase in lattice strain and the
96 reductions in crystallite size could be assigned to the peak broadening [19-21].

97 The comparison of SEM micrographs and the corresponding EDS microanalysis of pure $\text{TiO}_2\text{-C}$ and
98 $\text{TiO}_2\text{-M}$, $\text{TiO}_2\text{-M@G}$ composites at $4000\times$ are presented in figure 3a–c, respectively. It was found that
99 the milling process does not change the morphology of powders as well as the agglomeration of small
100 particles. It is confirmed by particle size distribution, presented in the insets of Figure 3b and a, that
101 mean particle size of the milled sample (~ 108 nm) is much smaller than that of $\text{TiO}_2\text{-C}$ without milling
102 (~ 143 nm). The micrographs illustrate that the particles have unequal sizes and do not have a well-
103 defined geometric morphology.

104



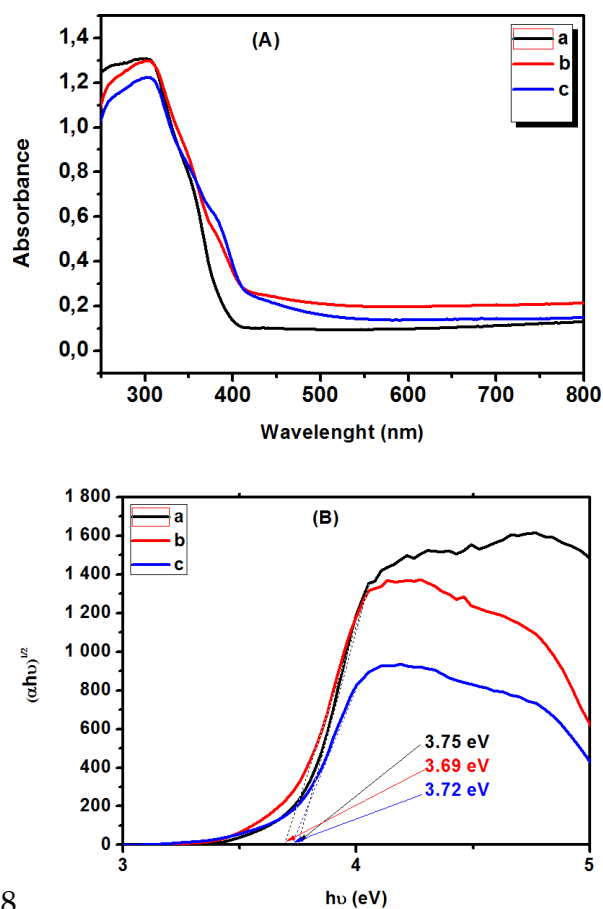
105
106

Figure 3. SEM images and EDS analysis of TiO₂-C (a), TiO₂-M (b) and TiO₂-M@G (c)

107 The composition of TiO₂-C, TiO₂-M, and TiO₂-M@G powders exhibits the lowest amount of oxygen
 108 (Ti:O ratio of 0.84), followed by TiO₂-M and then TiO₂-M@G (Ti:O ratio of 0.89-3.94 and 0.62-0.56,
 109 respectively). The EDS analysis does not show the presence of zirconia which confirms that the
 110 change of color (grey) is induced from oxygen vacancies and not from ball milling contamination.
 111 The high energy produced from ball milling in planetary ball mill produced from the collisions
 112 between balls and container wall, have an influence on TiO₂ powders. In addition, it could create
 113 some defects into TiO₂ structure. These defects and the interaction between neighboring crystallites
 114 at higher strains thereby resulting in a smaller crystallite size [22-24]. During annealing, Ti could be
 115 reduced into Ti₃O₅ (Ti_nO_{2n-1}) which are based on rutile with oxygen vacancies or into TiO_x where x < 2
 116 a mixed oxide of titanium.

117 Figure 4(A) and (B) exhibits the solid-state UV-Visible absorption spectra of TiO₂-C, TiO₂-M and TiO₂-
 118 M@G in the range of 200-800 nm and the corresponding Tauc plots, respectively. A small enhanced
 119 absorption was observed in the range of 350-800 nm. The absorption peak of TiO₂-C was located at
 120 312 nm, somewhat red-shifted for both TiO₂-M and TiO₂-M@G composite materials. Contrary to
 121 Dulian et al. [25], they reported that the increase of the absorbance of TiO₂ in the visible light is related
 122 to the addition of methanol in ball milling process. The band gaps extracted by plotting (αhν)^{1/2}
 123 versus photon energy (hν) using Tauc plot for pure TiO₂-C, TiO₂-M and TiO₂-M@G composite
 124 materials are presented in figure 4.

125



126

127

128

Figure 4. (A) UV-Visible absorbance and (B) Tauc plot of TiO₂-C (a), TiO₂-M (b) and TiO₂-M@G (c)

129 The measured bandgap for pure TiO₂ anatase was about ~3.2 eV which agrees with the literature
 130 value [26]. The appearance different band energies for TiO₂-C, TiO₂-M and TiO₂-M@G composite
 131 materials demonstrated the nature of the synthesized materials. Furthermore, as compared to pure
 132 TiO₂-C, a slight red-shift of ~0.07 and ~0.03 eV in the band edge position of TiO₂-M and TiO₂-M@G
 133 composite materials was observed, respectively. In the case of TiO₂-M, the influence of the ball milling
 134 process transformed partially the TiO₂ anatase to rutile phase is the credible reason for this effect. The
 135 high speed generated from grinding could increase the temperature and promote the reduction of
 136 TiO₂. The vacancy state turns as Ti³⁺ and or Ti⁴⁺ and creates new energy level just below the
 137 conduction band of the material [27].

138 4. Conclusions

139 In this paper, we have prepared anatase/rutile TiO₂ composite and anatase/rutile TiO₂@glucose
 140 composite using high energy ball milling process. This method could be a very efficient and leads to
 141 a decrease of particle size, phase transformation of TiO₂ partially from anatase to rutile and the
 142 absorption in the visible light. The suggested process is cost effective, ecofriendly and could be
 143 applied to prepare composites containing anatase-rutile TiO₂ and anatase-rutile TiO₂-glucose.

144 **Author Contributions:** "Imane Ellouzi. and Hicham Abou Oualid conceived and designed the experiments; I
 145 mane Ellouzi performed the experiments; Hicham Abou Oualid analyzed the data; Imane Ellouzi. wrote the
 146 paper. Hicham Abou oualid improve the discussion and edit the paper."

147 **Conflicts of Interest:** We declare that this manuscript is original, has not been reported before, and is not
 148 currently being considered elsewhere. We also confirm that there is no known conflict of interest regarding this
 149 manuscript and its publication. The manuscript has been approved by all named authors.

150 **References**

151

152 [1] Y. Wang, C. Sun, X. Zhao, B. Cui, Z. Zeng, A. Wang, G. Liu, and H. Cui, The Application of Nano-TiO₂ Photo
153 Semiconductors in Agriculture. *Nanoscale Res. Lett.* 11 (2016) 11: 529-535.

154 [2] J. Zhang, P. Zhou, J. Liu and J. Yu, New understanding of the difference of photocatalytic activity among
155 anatase, rutile and brookite TiO₂. *Phys. Chem. Chem. Phys.* 16 (2014) 20382-20386.

156 [3] Z. Sheng, Y. Hu, J. Xue, X. Wang, W. Liao, A novel co-precipitation method for preparation of Mn-Ce/TiO₂
157 composites for NO_x reduction with NH₃ at low temperature *Environ. Technol.* 33 (2012) 2421-2428.

158 [4] M. Polat, A. M. Soylu, D. A. Erdogan, H. Erguven, E. I. Vovk, E. Ozensoy, Influence of the sol-gel preparation
159 method on the photocatalytic NO oxidation performance of TiO₂/Al₂O₃ binary oxides. *Catal. Today.*
160 241 (2015) 25-32.

161 [5] M. Hosokawa, K. Nogi, M. Naito and T. Yokoyama, *Nanoparticle Technology*
162 *Handbook*. 1st ed. Elsevier, 2007.

163 [6] R. Ren, Z. Yang, and L. L. Shaw, Polymorphic transformation and powder characteristics of TiO₂ during high
164 energy milling, *J. Mat. Sci.* 35 (2000) 6015-2026.

165 [7] S. Begin-Colin, T. Giroit, G. Le Caër, and A. Mocellin, Kinetics and Mechanisms of Phase Transformations
166 Induced by Ball-Milling in Anatase TiO₂, *J. Solid State Chem.* 149 (2000) 41.

167 [8] X. Pan and X. Ma, Study on the milling-induced transformation in TiO₂ powder with different grain sizes.
168 *Mat. Lett.* 58 (2004) 513-515.

169 [9] X. Pan and X. Ma, Phase transformations in nanocrystalline TiO₂ milled in different milling atmospheres. *J.*
170 *Solid State Chem.* 177 (2004) 4098-4103.

171 [10] M. Uzunova-Bujnova, D. Dimitrov, D. Radev, A. Bojinova, and D.
172 Todorovsky, Effect of the mechanoactivation on the structure, sorption and photocatalytic properties of
173 titanium dioxide. *Mat. Chem. Phys.* 110 (2008) 291-298.

174 [11] P. Billik, G. Plesch, V. Brezov a, L'. Kuchta, M. Valko, and M. Maz ur, Anatase TiO₂ nanocrystals prepared
175 by mechanochemical synthesis and their photochemical activity studied by EPR spectroscopy, *J. Phys.*
176 *Chem. Solids* 68 (2007) 1112.

177 [12] S. B egin-Colin, A. Gadalla, G. L. Caë er, O. Humbert, F. Thomas, O. Barres, F. Villiéras, L. F. Toma, G.
178 Bertrand, O. Zahraa, M. Gallart, B. Honerlage, and P. Gilliot, On the Origin of the Decay of the
179 Photocatalytic Activity of TiO₂ Powders Ground at High Energy *J. Phys. Chem. C* 113 (2009) 16589-
180 16602.

181 [13] S. Yin, H. Yamaki, M. Komatsu, Q. Zhang, J. Wang, Q. Tang, F. Saito,
182 and T. Sato, Preparation of nitrogen-doped titania with high visible light induced photocatalytic activity
183 by mechanochemical reaction of titania and hexamethylenetetramine. *J. Mat. Chem.* 13 (2003) 2996-3001.

184 [14] Q. Zhang, J. Wang, S. Yin, T. Sato, and F. Saito, Synthesis of a visible-light active TiO₂-xS_x photocatalyst by
185 means of mechanochemical doping. *J. Am. Ceram. Soc.* 87 (2004) 1161-1163.

186 [15] J. Chen, G. J. Hirasaki, and M. Flaum, Effect of OBM on wettability and NMR responses *J. Pet. Sci. Eng.* 52
187 (2006) 161-171.

188 [16] C. Flood, T. Cosgrove, Y. Espidel, E. Welfare, I. Howell, and P. Revell, Fourier-Transform Carr-Purcell-
189 Meiboom-Gill NMR Experiments on Polymers in Colloidal Dispersions: How Many Polymer Molecules
190 per Particle?. *Langmuir* 24 (2008) 7875-7880.

191 [17] B. M. Madhusudan, H. P. Raju, S. Ghanaraja, Micro Structural Characterization and Analysis of Ball Milled
192 Silicon Carbide. *AIP Conference Proceedings* 1943, 020122 (2018); doi: 10.1063/1.5029698.

- 193 [18] J. Kim, J. Ho Chang, B.Y. Jeong, and J. Hyung Lee, Comparison of Milling Modes as a Pretreatment Method
194 for Cellulosic Biofuel Production Hyeon. *J. Clean Energy Technol.* , Vol. 1, No. 1, January 2013.
- 195 [19] LC. Damonte, LA. Mendoza Zelis, B. Mari Soucase, MA. Hernandez Fenollosa. Nanoparticles of ZnO
196 obtained by mechanical milling. *Powder Technol.* 148 (2004) 15–9.
- 197 [20] OM. Lemine, MA. Louly, AM. Al-Ahmari. Planetary milling parameters optimization for the production of ZnO
198 nanocrystalline. *Intern. J. Phys. Sci.* (2010) 2721–2729.
- 199 [21] A. Molladavoudi, S. Amir Khanlou, M. Shamanian, F. Ashrafizadeh, The production of nanocrystalline cobalt
200 titanide intermetallic compound via mechanical alloying. *Intermetallics* 29 (2012) 104–109.
- 201 [22] K. Lu K, J. Zhao, Equiaxed zinc oxide nanoparticle synthesis. *Chem Eng J* 160 (2010) 788–793.
- 202 [23] S. Ozcan , MM. Can, A. Ceylan, Single step synthesis of nanocrystalline ZnO via wet-milling. *Material*
203 *Letters* 64 (2010) 2447–2449.
- 204 [24] A.M. Glushenkov, H.Z. Zhang, Y. Chen, Reactive ball milling to produce nanocrystalline ZnO. *Mater Lett* 62
205 (24) (2008) 4047–4049.
- 206 [25] P. Dulian, M. Buras, W. Żukowski, Modification of photocatalytic properties of titanium dioxide by
207 mechanochemical method. *Polish J. Chem. Technol.* 3 (2018) 68–71.
- 208 [26] B. Aysin, A. Ozturk and J. Park, Silver-loaded TiO₂ powders prepared through mechanical ball milling,
209 *Ceramics Intern.* 39 (2013) 7119–7126.
- 210 [27] H. Khan and I. Khan Swat, Fe³⁺-doped Anatase TiO₂ with d–d Transition, Oxygen Vacancies and Ti³⁺ Centers:
211 Synthesis, Characterization, UV–vis Photocatalytic and Mechanistic Studies. *Ind. Eng. Chem. Res.* 55 (23)(2016)
212 6619–6633.
- 213
- 214

